International Journal of Chemical, Materials and Biomolecular Sciences
ISSN: 2415-6620
Vol:8, No:6, 2014

Generation of Catalytic Films of Zeolite Y and ZSM-5 on FeCrAlloy Metal

Rana Th. A. Al-Rubaye, Arthur A. Garforth

***Abstract*—**This work details the generation of thin films of structured zeolite catalysts (ZSM–5 and Y) onto the surface of a metal substrate (FeCrAlloy) using in-situ hydrothermal synthesis. In addition, the zeolite Y is post-synthetically modified by acidified ammonium ion exchange to generate US-Y. Finally the catalytic activity of the structured ZSM-5 catalyst films (Si/Al = 11, thickness 146 μm) and structured US–Y catalyst film (Si/Al = 8, thickness 23μm) were compared with the pelleted powder form of ZSM–5 and USY catalysts of similar Si/Al ratios.

The structured catalyst films have been characterised using a range of techniques, including X-ray diffraction (XRD), Electron microscopy (SEM), Energy Dispersive X–ray analysis (EDX) and Thermogravimetric Analysis (TGA). The transition from oxide-on-alloy wires to hydrothermally synthesised uniformly zeolite coated surfaces was followed using SEM and XRD. In addition, the robustness of the prepared coating was confirmed by subjecting these to thermal cycling (ambient to 550°C).

The cracking of n–heptane over the pellets and structured catalysts for both ZSM–5 and Y zeolite showed very similar product selectivities for similar amounts of catalyst with an apparent activation energy of around 60 kJ mol^{-1}. This paper demonstrates that structured catalysts can be manufactured with excellent zeolite adherence and when suitably activated/modified give comparable cracking results to the pelleted powder forms. These structured catalysts will improve temperature distribution in highly exothermic and endothermic catalysed processes.

***Keywords*—**FeCrAlloy, Structured catalyst, and Zeolite Y, Zeolite ZSM-5.

I. Introduction

THIN layers of zeolite catalyst have been coated on various metal substrates, including stainless steel, carbon and α–Al_2O_3, with the choice of substrate influencing the performance of the catalyst [1]. Metallic substrates such as FeCrAlloy have high mechanical resistance, high thermal conductivity and low pressure drop [2]. One of the major advantages of using FeCrAlloy is that the aluminium within it can be oxidised at high temperatures to form a thin surface film of aluminium oxide (Al_2O_3) [3], [4]. This oxide layer can then be used to anchor and subsequently grow zeolite phases [5].

Attachment of zeolite crystals on a metal surface to form a structured catalyst can be achieved using different methods with varying success. A dip coating uses a binder to attach already synthesised zeolite crystals to a (metal) surface. In-situ growth is a method of growing zeolite crystals onto the substrate using the alumina formed on the metal surface as a part source of Al required for the zeolite preparation [6]. The pre-treatment step is crucial as it requires the formation of a uniform thin aluminium oxide layer on the metal surface. This film then increases the wetting of the support by the synthesis gel mixture and/or promotes the nucleation of zeolite crystals [7]-[13].

The effect of both the FeCrAlloy pre-treatment and in-situ zeolite gel crystallisation time for zeolite Y and ZSM-5 film are reported here along with their catalytic performance for n-heptane cracking.

Rana Th. A. Al-Rubaye is a Lecturer in the Chemical Engineering Department, College of Engineering, University of Bagdad, Baghdad, Iraq (e-mail: Rana.Al-Rubaye@manchester.ac.uk).

Arthur A. Garforth is a Senior Lecturer and the Head of Teaching in the School of Chemical Engineering and Analytical Science, University of Manchester, Oxford Road, Manchester, M13 9PL, UK (e-mail: arthur.garforth@manchester.ac.uk).

II. Experimental

A. Support Pre-Treatment

FeCrAlloy annealed wires (0.5 mm diameter) were supplied by GoodFellows with a pre-determined chemical composition by weight of Fe 72.8%, Cr 22%, Al 5%, Y 0.1%, and Zr 0.1%.

The pre-treatment process was as follows; Oxide removeal using No.100 glass paper; immersion in 0.1M KOH at 25°C for 10 minutes, followed by 0.1M HNO_3 solution at 80◦C for 5min [13]. The wires were then rinsed with de-ionised water, placed in acetone and ultrasonicated for 10 minutes (Cam sonix C080T) and finally placed in de-ionised water and ultrasonicated for 10 minutes.

The wires were heated in a muffle furnace (Progen Scientific) to 1000°C in air at a heating rate of 10°C/ min and held at 1000°C for between 3–24 h. The wire samples were hung over a stainless steel support to ensure even oxidation of the surfaces and when removed from the furnace rapidly cooled to ambient temperature.

B. Preparing of the Structured Catalyst

The pre-treated FeCrAlloy support wires were cut into lengths (2.5 cm) and inserted vertically into a PTFE- lined autoclave and the hydrothermal zeolite synthesis performed.

ZSM–5 was synthesised using a seeding and feedstock gel [14], where a seeding gel with a molar composition of 4.5 Na_2O: 3.0 TPAOH: 60 SiO_2: 1200 H_2O was prepared using colloidal silica (Ludox AS–40 from Sigma–Aldrich), sodium hydroxide (Sigma–Aldrich) and tetrapropylammonium hydroxide (1M, Sigma–Aldrich). The seeding gel was aged overnight at 100°C and then 3.2g of the seeding gel was added to a feedstock with a molar composition of 6.5 Na_2O: 2 Al_2O_3: 60 SiO_2: 1916 H_2O. This was prepared by dissolving sodium aluminate (Fisher Scientific) and sodium hydroxide (Sigma–

Aldrich) in deionised water and adding colloidal silica (Ludox AS–40). The gel was then poured into a PTFE-lined autoclave, heated to 180°C in an oven and held at temperature for between 4–48 h.

The zeolite Y precursor solution was prepared from sodium aluminate (Fisher Scientific), colloidal silica (Ludox AS–40) and sodium hydroxide. The precursor solution (3.3 Na_2O: 0.75Al_2O: 10 SiO_2: 120 H_2O) was aged overnight at room temperature. The synthesis gel is then poured into a PTFE–lined autoclave and placed in the oven at 100°C for between 8–72 h.

After the hydrothermal synthesis, both the zeolite precipitated in the autoclave and the coated wires were removed, rinsed and then ultrasonicated in de-ionised water for 10 min.

In the case of ZSM–5, the powdered and the structured zeolite on FeCrAlloy support were heated in a muffle furnace (Carbolite Corp) from 25°C to 550°C at 1°C/min and held at 550°C for 16 hours to remove template. Then the as-made zeolite powders (1 g) and the structured zeolites were ion exchanged using a 0.5 M ammonium nitrate solution (NH_4NO_3, purity > 98% supplied by Sigma–Aldrich) at 80°C with constant agitation (60–100 rpm) for 1 hour. Finally filtered and then washed thoroughly with deionised water and dried at 100°C.

Post ion exchange the zeolite Y powder and structured zeolite had a 3 % Na content and were subjected to dealumination to produce the ultra-stable form of zeolite Y. The dealumination process was performed using acidified ammonia nitrate. The NH_4–Y powder or structured NH_4–Y zeolite were mixed with an ammonium nitrate solution (15% wt.) and the pH adjusted from 4.1 to 2.5 by the addition of HNO_3 (70% wt., supplied Camlab chemical, 0.4 g/g of exchanged zeolite). Then the slurry was heated to 85°C and held for 1 hour. Then the powder and structured Y zeolite were washed and dried at 100°C [15]. Finally, the dealuminated catalysts were ion exchanged once more following the procedure above to reduce the Na content to less than 0.5%.

III. Characterisation

The crystal growth of the zeolite on the wire surface was compared with the crystal growth in the bulk phase using a Philips X' Pert PRO X–ray diffraction scanning 0.000832°/min using slit widths 1/8° and 1/4° over a 2θ range of 3°–52°. The powder zeolite samples were analysed similarly except with a faster scanning rateof = 0.0289 °/min.

The calcination and adhesion of the zeolite layers for all samples was studied using a thermogravimetric analyzer (Q5000-IR TA Instruments). Calcination was carried out by heating in air (25 ml/min) from ambient at a rate of 1°C /min to 550°C and held at this temperature for 480 min. The adhesion of the zeolite layers was tested by thermal cycling selected wires between ambient to 550°C at 10°C/ min. The wires were held at both the high and low temperatures for 30 minutes and the process was repeated five times.

Surface morphology and chemical analysis were carried out on gold–coated powder and wires samples under high vacuum using the Quanta200 FEI scanning electron microscopy and the Genesis software.

Energy Dispersive Spectrometry EDS spectroscopy was used to identify elements and count the impinging X–rays based upon their characteristic energy levels [16]. Since, a well-polished surface is required for quantitative/qualitative analysis and concentration maps, two techniques were used. Firstly the external surface of the wire was analysed directly using X–ray spot analysis on carbon or gold–coated samples. Secondly the analysis of the elements dispersed across different layers of the metal, oxide layer and coated zeolite was carried out. Wires samples were prepared by immersion vertically in a resin and then sectioned with diamond saw to obtain a clean surface. This surface was then ground with SiC sandpaper and polished with Al_2O_3 to get a smooth flat surface. The samples were then rinsed with alcohol to remove contamination and finally carbon or gold–coated.

IV. Catalytic Crakinh Performance of Catalytic Films

The behavior of the structured and pelleted catalysts was studied using n–heptane cracking in a 4 mm i.d. quartz reactor. Bundles of the ZSM–5 and USY structured catalyst wires were loaded into the reactor (2.5 cm length x 0.05 cm diameter with a zeolite equivalent weight for ZSM–5 and Y of 0.04 and 0.03 gm, respectively). For comparison the same weight of pelleted ZSM–5 and USY zeolite catalyst (425–500μm pellets) were tested. The catalysts under test were sandwiched between two layers of quartz wool and the microreactor was located in the middle of the furnace (Carbolite MTF 12/12A). The catalysts were activated prior to n–heptane cracking by heating from 25°C to 550°C in air (1°C/min, 25 ml/ min) and held isothermally at 550°C for 16 hours. The n-heptane (99.99% Fluka) was supplied by flowing nitrogen through three bubblers connected in series and placed in an ice bath to maintain a constant temperature. All the stainless steel pipes connected between the reactor and the GC were lagged with heating wire (Electrothermal PLC, UK) and maintained at approximately 110°C to avoid any condensation of the reactant and products. A Varian 3400 FID GC fitted with a PLOT Al_2O_3/KCl capillary column (50m× 0.32 mm i.d.) was connected to the reactor and samples analysed at regular intervals between 5 and 125 min. All catalysts were studied at 450°C with a W/F= 42 g.h.mol^{-1} and the activity and selectivity reported.

V. Results

A. FeCrAlloy Substrate study

SEM analysis was carried out before and after each treatment step. Fig. 1 shows the surface of the wire magnified 240,000 times for the as supplied wire, sand–papered wire, the acid and caustic washed wire and, finally, the wire after all these treatments oxidised at 1000°C. The roughness of the surface increases after each pre–treatment step with an oxide

layer (Al_2O_3) observed on the FeCrAlloy surface after heating 4 h at 1000°C.

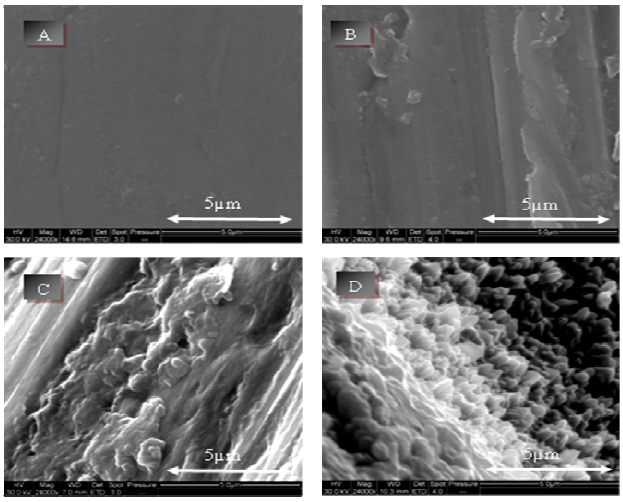

Fig. 1 SEM images of the FeCrAlloy wires before and after the physical pre-treated (A) as supplied, (B) sand-papered, (C) acid and base washed and (D) oxidised at 1000°C for 4 h

The weight of the wires increased after oxidation at 1000°C up to 4 hours (Table I) in good agreement with literature [17], [18]. Over the 24 h oxidation, the oxide layer first forms a continuous layer on which platelets develop, typically of γ–Al_2O_3 around 3–4 hours. These platelets transform to smoothened surfaces of α–Al_2O_3 (6+ hours) as highlighted in SEM images in Fig. 2 [19]-[21]. As might be expected elemental analysis showed the Cr and Fe is decreasing as the aluminium oxide layer develops (Al/Fe ratio increasing from 0.1 to 2.5) over the first 4 hours. However, after this time the Al/Fe ratio begins to decrease with prolonged oxidation time as seen by Badini [3].

TABLE I
THE WEIGHT GAIN, OXIDE LAYER THICKNESS AND ELEMENTAL ANALYSIS OF THE WIRE SURFACE AT DIFFERENT OXIDATION TIMES

Properites	0h	3h	4h	5h	6h	9h	24h
O (wt%)	0.0	49.0	48.0	44.6	51.8	48.9	44.7
Al (wt%)	8.8	52.0	58.6	45.9	39.7	25.1	54.7
Cr (wt%)	22.7	10.1	10.8	10.5	10.5	8.9	15.1
Fe (wt%)	68.5	24.7	27.0	23.8	23.0	16.7	41.4
Al/Fe Ratio	0.1	2.1	2.5	1.9	1.7	1.5	1.3
Oxide layer (µm)	0.0	2.0	4.1	3.4	2.8	2.1	2.5
Weight gain (g)	0.0	0.2	0.4	0.3	0.3	0.3	0.3

Prolonged oxidation time over 9 hours leads to a flat surface which eventually peels (24 hours) leaving areas of uneven oxide coating and revealing fresh iron/iron oxide beneath. This peeling suggests that the Al depletion has occurred at the interface of the oxide layer and the wire and hence the oxide layer is no longer bound and breaks off at prolonged oxidation times [3], [22].

Selected wires were studied using XRD and the development of alumina can be seen (Fig. 3) and is further confirmed by EDX mapping spectra taken through a cross-section of a wire oxidised for 4 hours (Fig. 4)

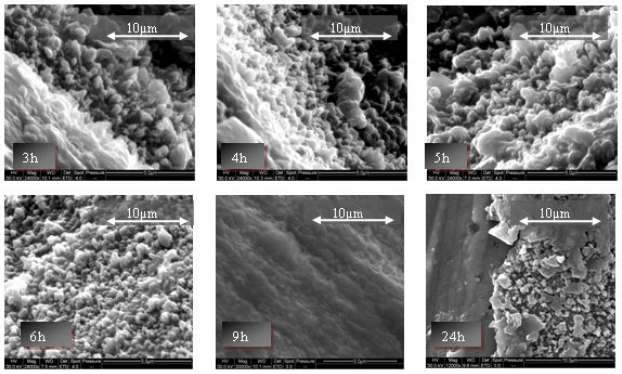

Fig. 2 Surface morphology of FeCrAlloy after different oxidation times

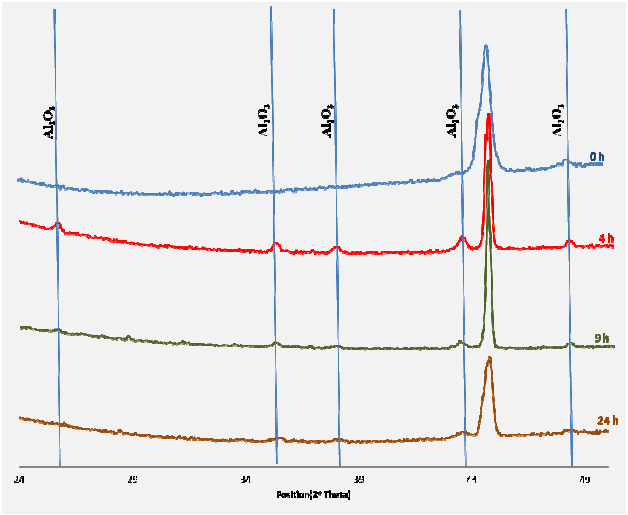

Fig. 3 XRD patterns for pre-treated wires at different oxidation time (0, 4, 9 & 24 h)

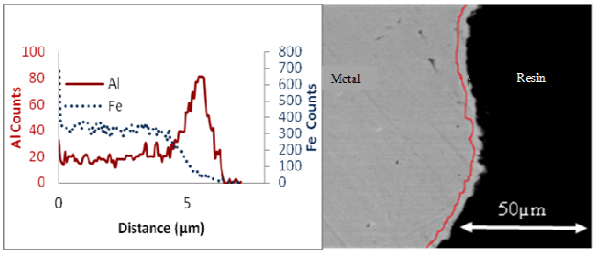

Fig. 4 Elemental line scans cross the wires oxidised at 1000°C, 4h (for clarity, the red line approximates the position of oxide layer)

B. Preparation of Structured Catalysts

1. Optimisation of Wire Oxidation Time and Subsequent Zeolite ZSM-5 Coating

Wires oxidised at 1000°C for between 3–24 h were then immersed in aged zeolite ZSM–5 gel and heated. A uniform layer of ZSM-5 covered the oxidised wires (SEM analysis Fig.

5). All coated wires were calcined and thermal cycled in a TGA to determine adhesivity of zeolite films on the substrate surface and the zeolite coverage (g/m^2) was estimated by taking the increase in the mass of the wire due to the growth of the zeolite film and dividing by the The morphology of ZSM–5 on the oxidised wires was investigated after calcination (Fig. 5) and found to be similar for all wire oxidation timescales however evidence of slower growth of ZSM–5 can be seen when the oxide layer has a much lower surface area (i.e. > 6 h).

Thermal cycling had little obvious effect on morphology but the zeolite layer began to peel off wires oxidised for 6 h or more. The damaged ZSM–5 surface grown on the 24 h oxidised wire is highlighted in Fig. 6.surface area of the wires (Table II).

All wires lost weight on heating to 550°C due to the breakdown of structure-directing template, TPAOH. Thermal cycling of the wires which had been oxidised for 3–5 h showed very little weight loss (0.1%). However, wires oxidised for 6 h showed a 10-fold increase in weight loss and wires oxidised for 9 hours or more showed significant peeling of the zeolite layer. A significant increase in coverage and excellent adherence on thermal cycling suggest the wire oxidation time at 1000°C is optimum at 4 hours.

TABLE II
THE CHANGE IN ZSM–5 COVERAGE OF WIRES OXIDISED BETWEEN 3 – 24H AND THE WEIGHT CHANGE AFTER CALCINATION AND THERMAL CYCLING

Wires	3h	4h	5h	6h	9h	24h
Zeolite coverage (g/m^2)	192	317	161	151	142	102
Weight loss on calcination (%)	3.4	3.2	2.5	2.0	1.9	1.8
Weight loss after thermal cycling×5(%)	0.1	0.1	0.1	1.0	7.8	10.9
Thickness Layer (μm)	130	150	125	120	80	51

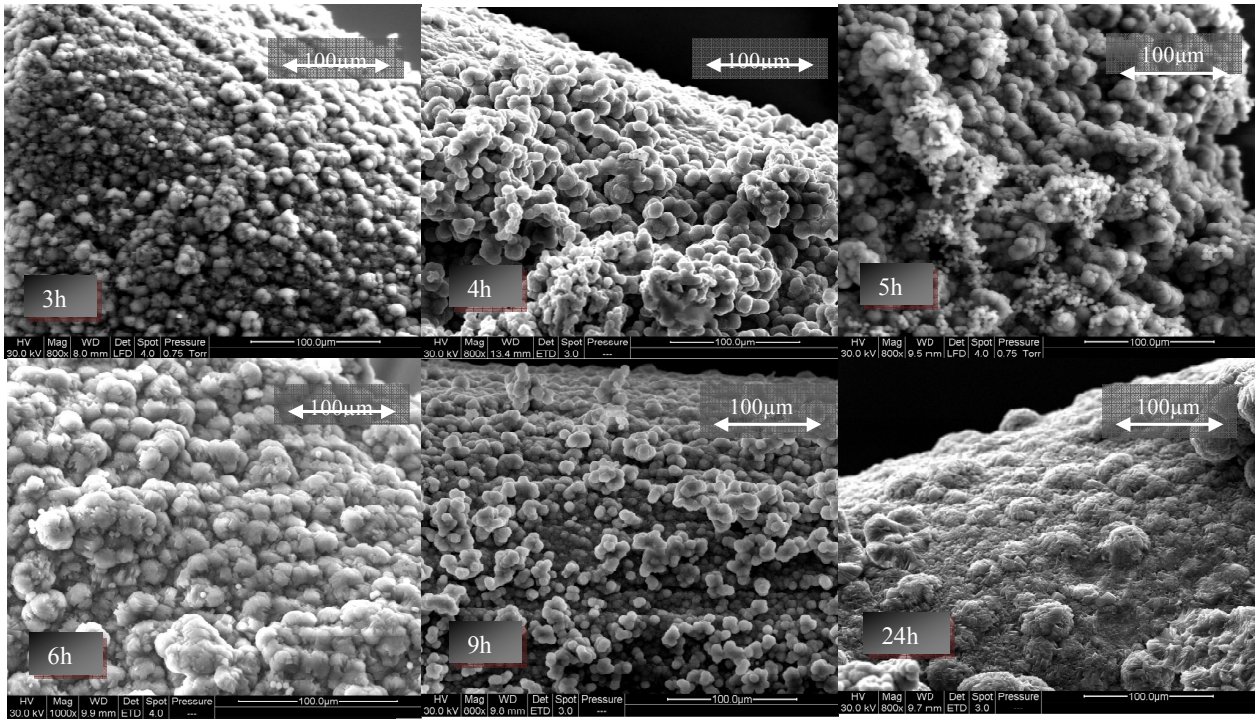

Fig. 5 SEM images showing the morphology of ZSM–5 grown on wires oxidised for between 3 –24 hours

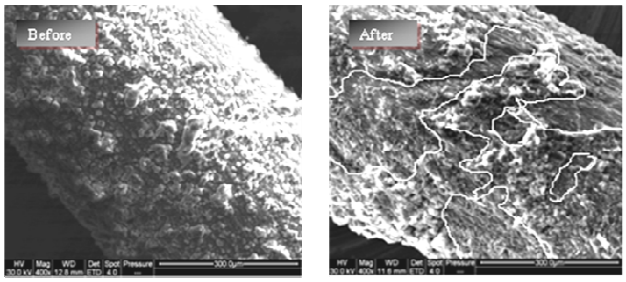

Fig. 6 SEM images before and after thermal cycling for ZSM–5 coated wires oxidised for 24 h. Note the highlighted area where peeling has occurred

2. Optimisation of Wire Oxidation Time and Subsequent Zeolite Y Coating

The hydrothermal synthesis of zeolite Y on wires oxidised for between 3–24 h was carried out to study the effect of both the substrate oxidation time on the catalyst loading and thermal stability of the structured catalysts. SEM images of wires oxidised for between 3–24 h coated with zeolite Y are shown in Fig. 7 and there was little change in the morphology. However, unlike the ZSM–5, zeolite Y coverage of the surface was uneven and more difficult to achieve with thinner layers (Table III).

The entire weight loss from the zeolite film on the wires on calcination was due to H_2O being removed from the zeolite.

Again the wires oxidised for 4 hours showed the largest growth of zeolite and again good adhesion of zeolite Y on the substrate surface on thermal cycling for wires oxidised up to 5 hours.

Similar to ZSM–5 on thermal cycling, Zeolite Y began to peel from the wires oxidised for 6 h and above and the damaged surface of the coated wire oxidised for 24 hours is shown in Fig. 8. Again the optimum wire oxidation time for best zeolite growth and adhesion was 4 hours.

The synthesis conditions for zeolite Y and ZSM–5 were quite different for example zeolite Y was synthesised at 100°C whilst ZSM–5 was 180°C. The Si/Al ratio of the gel composition was also significantly different and therefore the interaction with the aluminum oxide layer on the FeCrAlloy wire for both syntheses will be different [23], [24]. For example, a low Si/Al ratio in the zeolite gel composition will lead to decrease in the nucleation and growth rates [25]. The aluminium oxide scales observed at 1000°C help with seeding the zeolite on the support surface [2]. In addition, the roughness of the surface although different for each wire and hence the number of the nucleation sites may vary, this is not the most likely reason for the slower growth in zeolite Y [9].

TABLE III
THE CHANGE IN ZEOLITE Y COVERAGE OF WIRES OXIDISED BETWEEN 3H – 24H AND THE WEIGHT CHANGE AFTER CALCINATION AND THERMAL CYCLING

Wires	3h	4h	5h	6h	9h	24h
Zeolite coverage (g/m^2)	52	57	51	24	20	10
Weight loss on calcination (%)	1.5	1.5	1.1	0.9	0.2	0.2
Weight loss after thermal cycling×5(%)	0	0	0	0.2	1.4	2.2
Thickness Layer (μm)	20	23	20	20	8	2

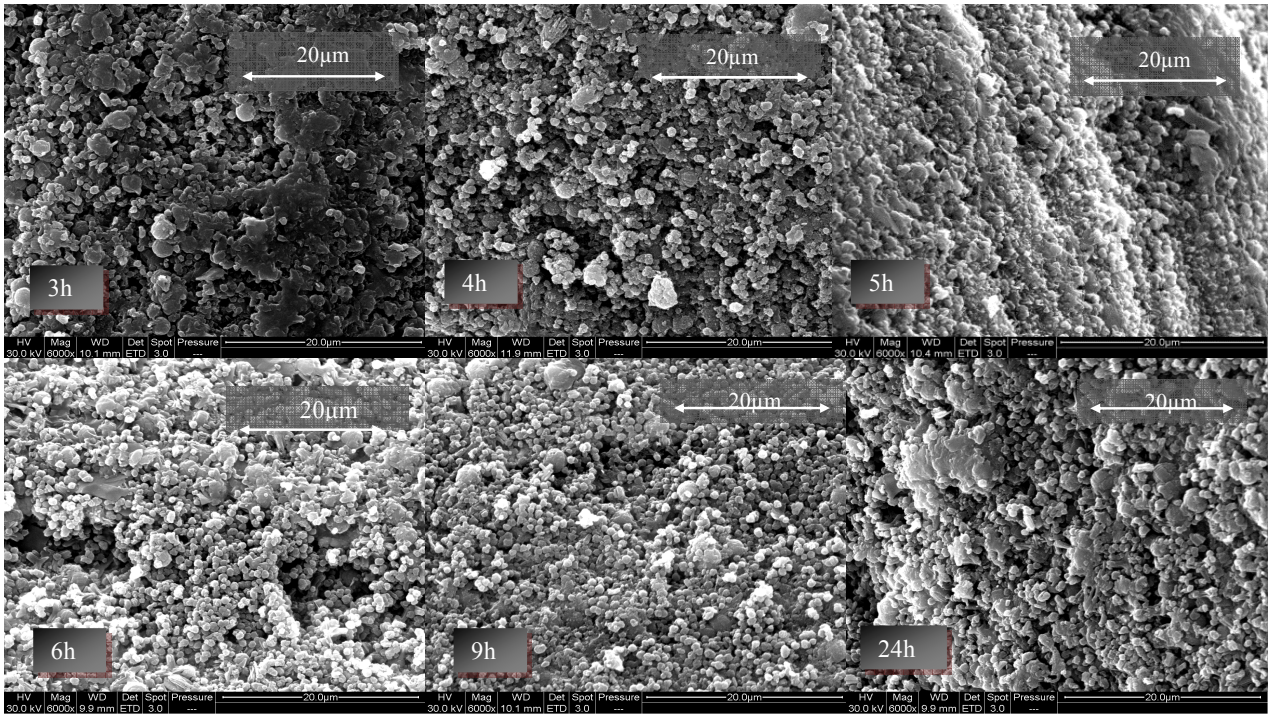

Fig. 7 SEM images of zeolite Y on the surface of wires oxidised for different times

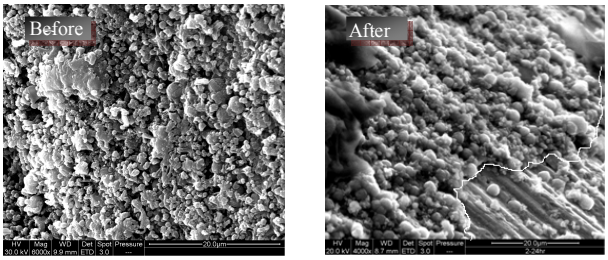

Fig. 8 SEM images before and after thermal cycling for zeolite Y coated wires oxidised for 24 h. Note the highlighted area where peeling has occurred

3. Optimisation of the Zeolite Crystallisation Time ZSM–5 Structured Catalyst

The hydrothermal synthesis of ZSM–5 was carried out at different crystallisation times by immersing the FeCrAlloy wires oxidised for 4 h. In order to study the growth of the zeolite on the metal surface, the analyses were performed on the zeolite in the bulk phase and on the zeolite grown on the metal surface.

XRD was performed to study the crystal growth of the zeolite on the wire surface and compared with the crystal growth in the bulk phase. These analyses confirm that the increase in crystallisation time leads to an increase in the intensity of the XRD peaks of ZSM–5. It is worth noting that ZSM–5 crystallisation starts earlier on the alumina-rich metal

surface (12 h) whilst forming slower in the bulk (typically 20 h, Fig. 9). This suggests that the crystallisation is assisted by the alumina layer formed on the FeCrAlloy surface. The crystallisation was complete by 48 h for both the bulk powder and the FeCrAlloy wires.

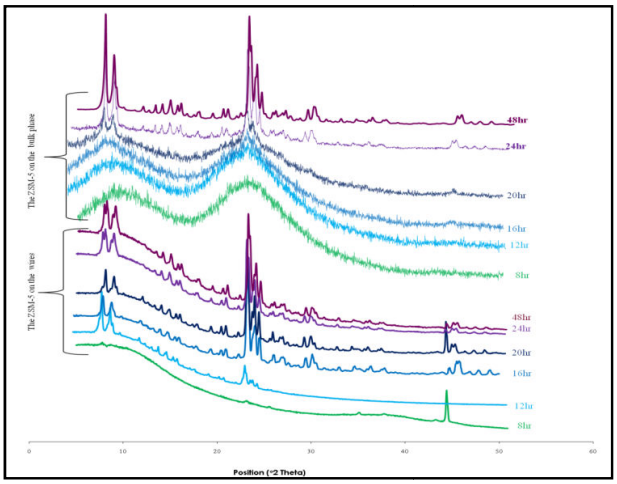

Fig. 9 XRD patterns as ZSM–5 is crystallised on the metal surface and in the bulk phase

SEM images were taken of the wires surface at different crystallisation times and revealed differences in the zeolite coverage as well as crystal size. Initially growth was on FeCrAlloy wire surface then the crystals subsequently grow on other crystals already present.

Good coverage at crystallisation times of 12, 20 and 48 h showed spherical crystals with twining. As might be expected as the crystallisation time increased so did the surface coverage and the typical Si/Al ratio achieved was 11 (Table IV). A similar Si/Al ratio was found for the bulk ZSM-5 powder.

TABLE IV
ZSM-5 WEIGHT GAIN, LAYER THICKNESS AND SI/AL RATIO AT DIFFERENT CRYSTALLISATION TIMES

Time (h)	Zeolite (%)	Layer thickness (μm)	Coverage (g/m^2)	Si/Al
4	0.03	5	0.25	0.03
8	1.8	10	16	8.00
12	11.3	50	100	11.21
16	15	100	151	11.15
20	18	120	152	11.04
24	23	134	212	11.02
48	35	146	317	11.00

Element mapping for Na-ZSM-5 structured catalyst after 48 h crystallisation time is shown in Fig. 10 (a). Fe and Cr mapping clearly showed the elements present in the body of the wire and Si and Al clearly show the zeolite grown on the wire. The Al mapping showed a very sharp increase in Al concentration at the surface of the wire (bright red line signifying the boundary between the wire and the zeolite). This is also highlighted in the line scan of the cross-section of the wire on Fig. 10 (b). The Kα signals plotted of Si, Al, Fe and Cr started where the EDAX elemental line scan was made on the chosen range to show the structure catalyst structure (substrate, aluminium oxide layer, zeolite layer). The Cr and Fe from the FeCrAlloy wire is not zero due to the background signal. The sharp peak in Al Kα signals plotted indicated the aluminium oxide layer on the metal surface then the signal decreases

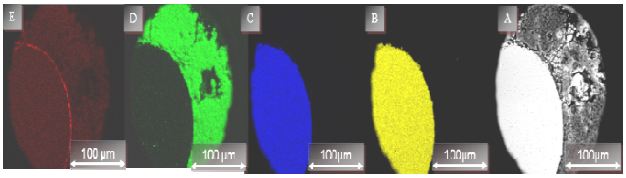

Fig. 10 (a) SEM-EDAX micrograph of the Na-ZSM-5 structured catalyst after 48 h crystallisation time: A) BSE image, (B, C, D and E) element mapping for Fe, Cr, Si and Al respectively

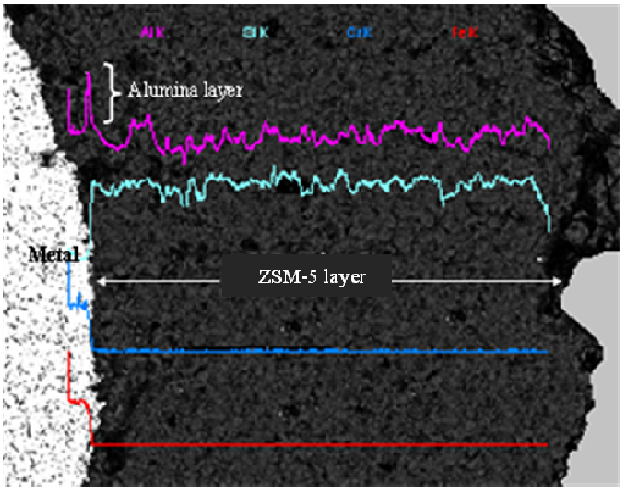

Fig. 10 (b) Line scan of cross-section through the wire, alumina and zeolite phase; purple line, light blue line, blue line, and red line represent the Al, Si, Cr, and Fe, respectively (after 48 h crystallisation time)

The element mapping through the cross-section also highlights defects such as cracks and one large cavity within the zeolite phase. Overall the zeolite phase is continuous and attached but further improvements in synthetic method will improve homogeneity of the zeolite coating.

4. Optimisation of the Zeolite Crystallisation Time Zeolite Y Structured Catalyst

Following the growth of zeolite Y on the wires by XRD was challenging due to the slow growth rate, but the typical reflection of the low angle (2θ = 6.1 – 10.4o) for the zeolite Y was noticeable after 16 hours. XRD pattern of zeolite Y on the wire showed the presence of other phases after 72 hours (potentially GIS, GME, CHA, Fig.11). The pure crystalline phase of zeolite Y with no amorphous material was formed in the bulk at 72 h.

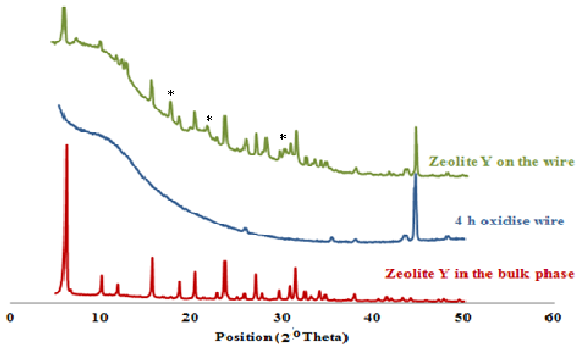

Fig. 11 XRD patterns of Zeolite Y synthesis after 72h on the wire oxidised for 4 h, the XRD pattern of the wire after 4h oxidation and finally the bulk phase. Impurities in the zeolite Y phase are highlighted (*)

SEM images (not shown here) at 8 h showed the oxidised aluminum oxide platelets/whiskers however by 16 h, the surface is smooth with a predominantly amorphous layer present. XRD analysis suggests the beginning of the formation of seeds of zeolite Y because of the appearance of a typical reflection at low angle ($2\theta = 6.1 - 10.4^{o}$). After 24 h, zeolite crystals appeared on the surface and the crystallisation was complete after 72 h with crystals being of a similar size and morphology as the zeolite produced in the bulk phase.

Study of the cross-section of the wires showed an increase in layer thickness and surface coverage achieved with crystallisation time (Table V) and a final Si/Al ratio was between 2.72 and 2.76 (from EDAX). The limit in the layer thickness around 21 µm suggests a combination of zeolite growth followed by dissolution taking place.

TABLE V
ZEOLITE NA-Y WEIGHT GAIN, LAYER THICKNESS AND SI/AL RATIO AT DIFFERENT CRYSTALLISATION TIMES

Zeolite Y Film Properties	8h	16h	24h	32h	40h	48h	72h
Zeolite coverage (g/m^2)	10	11	19	25	48	51	58
Zeolite (%)	1.2	1.2	2.1	2.8	5.4	5.7	6.4
Thickness Layer (µm)	1.5	3.7	4.4	8.7	20	21	23
Si/Al	2.7	2.7	2.7	2.7	2.7	2.7	2.7

EDAX elemental line scans a cross the wire and zeolite layer after 72 h is shown in Figs. 12 (a) & (b). Unlike the ZSM–5, the zeolite Y layer was thinner and only 23 µm in thickness. Again, Kα Si, Al, Fe and Cr signals plotted across the wire, aluminium oxide layer and zeolite layer. The Al peak was observed confirming the presence of aluminium oxide layer on FeCrAlloy surface and is also shown in Fig. 12 (a). As was the case with ZSM–5, there were defects but the zeolite layer did not appear to be as homogeneous with areas of high concentrations of Si noted, suggesting the synthesis would have benefitted from agitation. In addition, there was a noticeably broader and uneven concentration of the Al at the boundary of the wire and the zeolite growth.

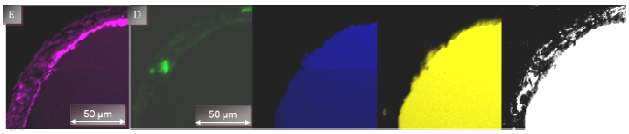

Fig. 12 (a) SEM–EDAX micrograph of the Na–Y structured catalyst crystallised after 72 h: A) BSE image and B, C, D and E show element mapping for Fe, Cr, Si and Al respectively

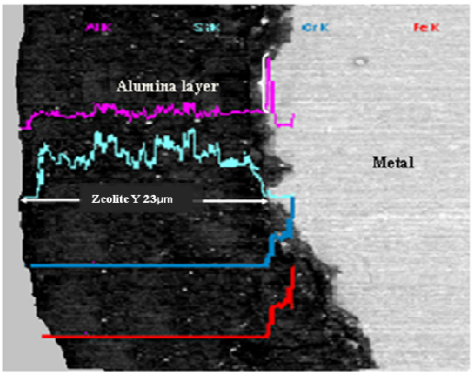

Fig. 12 (b) SEM images of zeolite Y coverage at 72 h on structured catalyst

C. Catalyst Testing Using N-Heptane Cracking in a Fixed Bed Reactor

1. ZSM–5 Pelleted and Structured Catalyst

The catalytic activity of ZSM–5 pellets (250–425µm) and bundles of structured ZSM-5 catalyst grown on wires was determined using n-heptane cracking in a fixed bed micro–reactor. The conversion of n–heptane for an equivalent amount of catalyst at 450°C and W/F= 42 g.h. mol^{-1} is shown in Fig. 13. Neither catalyst showed deactivation although a lower conversion was observed over the structured catalyst. The most likely explanation being the poorer packing of the wires compared to that of the pellets. This poorer packing could result in channelling or effectively shorter contact times and hence lower conversion. Importantly the selectivity of the two catalysts is similar showing subtle differences in yields related to residence time (Fig. 14). The apparent activation energy was determined around 60 kJ mol^{-1} for both catalysts indicating surface reaction kinetics predominate.

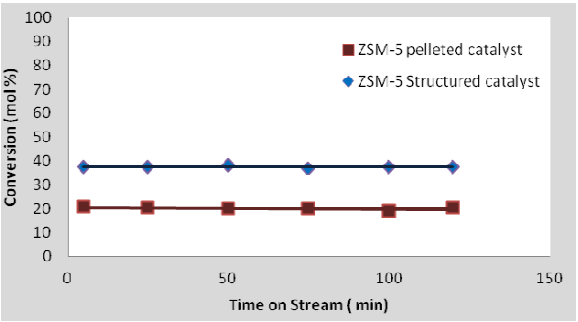

Fig. 13 Conversion of n-heptane over pelletted and structured ZSM-5 at 450°C

Both catalysts produced around 23–25 mol/100mols converted of propene ($C_3^=$) and 16–19 mol/100mols converted butenes ($C_4^=$). The amount of secondary products was not unsurprisingly higher in the pelleted catalyst with approximately twice the mol/100mols converted of propane (C_3) and iso-butane (iC_4) generated.

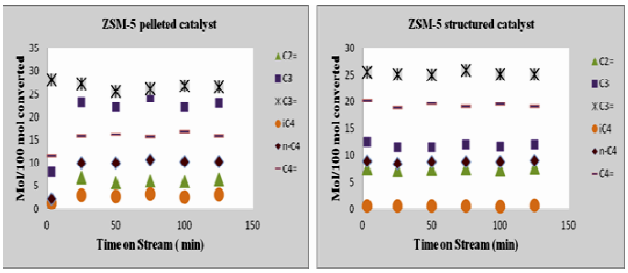

Fig. 14 Selectivity with time for key products for pelletted and structured ZSM-5 at 450°C

2. Pelleted and Structured Y Catalyst

The Si/Al ratio for post synthetically modified powder and structured zeolite Y structured increase of from 2.7 to approximately 8 (as determined by MAS NMR).

The catalytic activity of Y pellets (250 – 425µm) and bundles of structured Y catalyst grown on wires was determined and the conversion of n–C_7 for an equivalent amount of catalyst at 450°C and W/F= 42 g.h .mol^{-1} is shown in Fig. 15. As expected both catalysts deactivate rapidly with the pelletted Y catalyst showing the greater activity.

Despite the higher conversion of the pelleted Y catalyst, the product selectivities of both catalysts at 450°C were quite similar (Fig. 16) with $C_3^=$ and $C_4^=$ the major products with neglible amounts of C_1 and C_5. The strongest sites deactivate first and hence there was a rapid decrease in i–C_4 production accompanied by a rapid increase in $C_3^=$ and $C_4^=$ with time [25]. Both catalysts behaved similarly and not too surprisingly apparent activation energy of approximately 60 kJ mol^{-1} was determined for both.

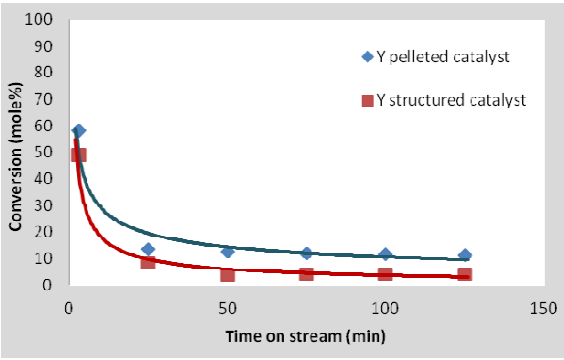

Fig. 15 Conversion of n-C7 cracking for pelleted and structured Y at 450°C

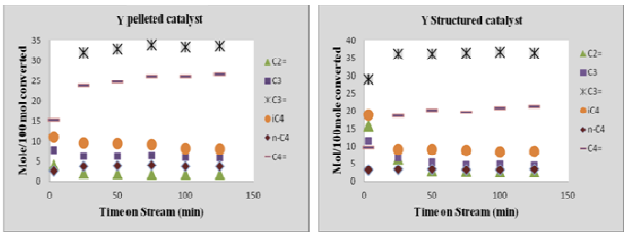

Fig. 16 Selectivity of n–C7 cracking for pelleted and structured Y at 450°C with time

VI. Discussion and Conclusions

Coatings grown on physically pre-treated wires oxidised at 1000°C for a time of 3–5 hours were optimal. Both ZSM–5 (48 hours at 180°C, Si/Al = 11) and zeolite Y (72 hours at 100°C, Si/Al = 2.7) were successfully synthesised on FeCrAlloy wires that had been oxidised for 4 hours. In both cases, a continuous zeolite layer was successfully anchored to the alumina grown on the surface of the wire during oxidation, Zeolite Y growth was more problematic with a much thinner and more heterogeneous layer produced. Zeolite Y was the predominant phase (XRD) but areas of high Si concentration and structural flaws were observed using SEM. Repeated thermal cycling of both structured catalysts showed the zeolite coatings to be stable with little flaking or loss of catalyst layer. However, the synthesis of zeolites on wires oxidised for greater than 5 hours were prone to flaking and loss of layer integrity.

Finally n–C_7 cracking revealed lower cracking activities for both the structured catalysts with the most likely explanation being the imperfect packing of the fixed bed micro-reactor which allowed some degree of channelling of the reactant resulting in lower conversions. Despite the drawback, both ZSM–5 (Si/Al = 11) and the acid-leached zeolite Y (Si/Al = 8) structured catalysts showed similar product selectivities to their pelleted counterparts. Increased i–C_4 yields indicated more secondary reactions in the case of the pelleted catalysts supporting the lower activity observed for the structured catalysts. Apparent activation energies of approximately 60 kJmol^{-1} for all catalysts suggested similar reaction mechanisms and that the surface reaction was controlling.

Further work is continuing optimising the synthesis of zeolite Y and on improving the flow patterns through the packed bed reactor using a larger diameter reactor with increased catalyst bundles.

Acknowledgements

We gratefully thank the staff in the School of Chemical Engineering and Analytical Science (CEAS) at University of Manchester, in particular to Dr. Patrick Hill (CEAS) and Dr. Christopher Muryn (Chemistry) for training and support on SEM and XRD analyses. Dr Aaron Akah and Miss Chandni Rallan for their laboratory support, and the University of Bagdad, Iraq, for their financial support.

REFERENCES

[1] Jansen, J., et al., Zeolitic coatings and their potential use in catalysis. Microporous and Mesoporous Materials, 1998. 21(4): p. 213-226.
[2] Zamaro, J.M., M.A. Ulla, and E.E. Miró, ZSM-5 growth on a FeCrAl steel support. Coating characteristics upon the catalytic behavior in the NOxSCR. Microporous and Mesoporous Materials, 2008. 115(1): p. 113-122.
[3] Badini, C. and F. Laurella, Oxidation of FeCrAl alloy: influence of temperature and atmosphere on scale growth rate and mechanism. Surface and coatings technology, 2001. 135(2): p. 291-298.
[4] Samad, J.E., J.A. Nychka, and N.V. Semagina, Structured catalysts via multiple stage thermal oxidation synthesis of FeCrAl alloy sintered microfibers. Chemical Engineering Journal, 2011. 168(1): p. 470-476.
[5] Yuranov, I., A. Renken, and L. Kiwi-Minsker, Zeolite/sintered metal fibers composites as effective structured catalysts. Applied Catalysis A: General, 2005. 281(1): p. 55-60.
[6] Meille, V., Review on methods to deposit catalysts on structured surfaces. Applied Catalysis A: General, 2006. 315: p. 1-17.
[7] Munoz, R., et al., Zeolite Y coatings on Al-2024-T3 substrate by a three-step synthesis method. Microporous and Mesoporous Materials, 2005. 86(1): p. 243-248.
[8] Wang, Z., J. Hedlund, and J. Sterte, Synthesis of thin silicalite-1 films on steel supports using a seeding method. Microporous and Mesoporous Materials, 2002. 52(3): p. 191-197.
[9] Mintova, S., V. Valtchev, and L. Konstantinov, Adhesivity of molecular sieve films on metal substrates. Zeolites, 1996. 17(5): p. 462-465.
[10] Wu, X., et al., Influence of an aluminized intermediate layer on the adhesion of a γ-Al2O3 washcoat on FeCrAl. Surface and coatings technology, 2005. 190(2): p. 434-439.
[11] Valentini, M., et al., The deposition of γ-Al_2 O_3 layers on ceramic and metallic supports for the preparation of structured catalysts. Catalysis today, 2001. 69(1): p. 307-314.
[12] Mies, M., et al., Hydrothermal synthesis and characterization of ZSM-5 coatings on a molybdenum support and scale-up for application in micro reactors. Catalysis today, 2005. 110(1): p. 38-46.
[13] Alrubaye, R.T.A., B. Atilgan, R. J. Holmes, and A. A. Garforth, Growing Zeolite Y on FeCrAlloy Metal. World Academy of Science, Engineering and Technology, 2013(76): p. 889-893.
[14] Chou, Y.H., et al., Mesoporous ZSM-5 catalysts: Preparation, characterisation and catalytic properties. Part I: Comparison of different synthesis routes. Microporous and Mesoporous Materials, 2006. 89(1): p. 78-87.
[15] Vassilakis, J.G. and D.F. Best, Novel zeolite compositions derived from zeolite Y. US Patent 5,013,699, 1991 - 1991, Google Patents.16. Danilatos, G., Review and outline of environmental SEM at present. Journal of Microscopy, 2011. 162(3): p. 391-402.
[16] Kadiri, H.E., et al., Abnormal high growth rates of metastable aluminas on FeCrAl alloys. Oxidation of metals, 2005. 64(1): p. 63-97.
[17] Camra, J., et al., Role of Al segregation and high affinity to oxygen in formation of adhesive alumina layers on FeCr alloy support. Catalysis today, 2005. 105(3): p. 629-633.
[18] Richardson, J.T., Principles of catalyst development. 1989. p. 70 - 120: Springer.
[19] Kochubey, V., Effect of Ti, Hf and Zr additions and impurity elements on the oxidation limited lifetime of thick-and thin-walled FeCrAlY-components. 2005, PhD thesis, Ruhr-Universität Bochum, Universitätsbibliothek.
[20] Huntz, A., et al., Thermal expansion coefficient of alumina films developed by oxidation of a FeCrAl alloy determined by a deflection technique. Applied surface science, 2006. 252(22): p. 7781-7787.
[21] Herbelin, J.M. and M. Mantel, Effects of Al addition and minor elements on oxidation behaviour of FeCr alloys. Le Journal de Physique IV, 1995. 5(C7): p. 7-7.
[22] Bhatia, S., Zeolite catalysis: Principles and applications. 1990, CRC Press (Boca Raton, Fla.).
[23] Rebrov, E.V., et al., Hydrothermal Synthesis of Zeolitic Coatings for Applications in Micro-structured Reactors. Ordered Porous Solids: ecent Advances and Prospects, 2008: p. 311.
[24] Persson, A., et al., Synthesis of stable suspensions of discrete colloidal zeolite (Na, TPA) ZSM-5 crystals. Zeolites, 1995. 15(7): p. 611-619.
[25] Jacobs, P.A. and J.A. Martens, Introduction to acid catalysis with zeolites in hydrocarbon reactions. Studies in Surface Science and Catalysis, 1991. 58: p. 445-496.